



Galloway, J., Talbot, J., Critchley, K., Miles, J., & Bramble, J. (2015). Developing Biotemplated Data Storage: Room Temperature Biomineralization of L10 CoPt Magnetic Nanoparticles. *Advanced Functional Materials*, 25(29), 4590-4600. <https://doi.org/10.1002/adfm.201501090>

Peer reviewed version

Link to published version (if available):
[10.1002/adfm.201501090](https://doi.org/10.1002/adfm.201501090)

[Link to publication record on the Bristol Research Portal](#)
PDF-document

University of Bristol – Bristol Research Portal

General rights

This document is made available in accordance with publisher policies. Please cite only the published version using the reference above. Full terms of use are available: <http://www.bristol.ac.uk/red/research-policy/pure/user-guides/brp-terms/>

ADVANCED FUNCTIONAL MATERIALS

Supporting Information

for *Adv. Funct. Mater.*, DOI: 10.1002/adfm.201501090

Developing Biotemplated Data Storage: Room Temperature
Biom mineralization of L1₀ CoPt Magnetic Nanoparticles

Johanna M. Galloway, Jennifer E. Talbot, Kevin Critchley,
Jim J. Miles, and Jonathan P. Bramble*

Supporting Information for: Developing Biotemplated Data Storage: Room Temperature Biomineralization of L1₀ CoPt Magnetic Nanoparticles

J. M. Galloway, J. E. Talbot, K. Critchley, J. J. Miles, and J. P. Bramble*

Detailed Experimental Methods

Substrate Preparation: A silicon wafer was sectioned into 1 cm squares and cleaned with propanol, soaked in ethanol (1 hour), dried with N₂, then treated with UV/ozone for 20 minutes (UVOCS). Poly dimethyl siloxane (PDMS) was mixed thoroughly (Sylguard 184 base with 10% curing agent (w/w), Dow Corning), degassed under vacuum and poured over the silicon master before curing (60°C, 16 hours). Stamps were cut out, soaked in ethanol (20 minutes) before treating with UV/ozone (20 minutes) to create a hydrophilic surface. The stamp was inked with a 1 mg mL⁻¹ solution of the CoPt_DAP peptide (Ac-HPPMNASHPHMH-GSG-KTHEIHSPLLHK-Am, from Genscript, >95% purity, *N*-terminal acetylation, *C*-terminal amidation) in phosphate buffered saline (PBS, Invitrogen: 10 mM sodium phosphate, 2.68 mM KCl, 140 mM NaCl, pH 7.4). After a minute, excess peptide solution was removed via pipette, and the stamp gently dried with a stream of N₂. This process was repeated up to 10 times to thoroughly ink the stamp with the peptide. As the behavior of the ink used in micro-contact printing can be affected by the surrounding humidity and temperature, the number of inking and drying rounds may need to be optimized for different peptides and different ambient laboratory conditions.^[1] The stamp was then conformally contacted onto silicon (cleaned as for the stamp above) for one minute before being removed, and the stamped substrate placed in a glass reaction vessel. The native oxide layer created on the clean silicon during cleaning provides a key for the SiO₂ binding portion of the peptide, allowing the DAP to transfer to the silicon surface from the inked stamp.

Mineralization: Aqueous stocks of cobalt (Co²⁺, 30 mM CoSO₄·7H₂O, Sigma Aldrich, (99.998%), 126.5 mg in 15 mL) and platinum (Pt²⁺, 10 mM Na₂PtCl₄, Alfa Aesar (99.99% Premion), 57.4 mg in

15 mL) salts, and a reducing agent (sodium borohydride, 25 mM, NaBH₄, Alfa Aesar (>98%), 28.5 mg in 30 mL) were prepared in deoxygenated MilliQ water (vacuum degassed for >1 hour and N₂ sparged for >1 hour before use). Via ports in the reaction vessel, 2.5 mL Co²⁺ and 2.5 mL Pt²⁺ were added to the peptide coated silicon substrate and incubated for 5 minutes at room temperature. For the bulk peptide control, 100 μL of the 1 mg mL⁻¹ peptide solution (10 μg L⁻¹ in the 10 mL reaction) in PBS was added to the metal salts in the reaction vessel in place of the peptide incubated substrate. N₂ was flowed through the solution in the reaction vessel to both mix the reaction and maintain anoxia of the reaction solution. 5.0 mL of NaBH₄ was then injected into the reaction vessel and N₂ flow maintained. The yellow-pink salt solution is reduced to black metallic nanoparticles, both in the bulk solution and onto the peptide immobilized on the silicon substrate. After 45 minutes, biotemplated surfaces were removed from the excess reactants and products, and rinsed 3-5 times in deoxygenated water and dried with N₂.

Electron Microscopy: A Hitachi SU8230 cold field emission (CFE) scanning electron microscope (SEM) was used to image samples mounted onto aluminum stubs at 2-10 keV via the in lens SE (U) detector. Energy dispersive X-ray (EDX) spectra were recorded using an Oxford Instruments AZtecEnergy EDX system on the SEM at 5 keV. Transmission electron microscopy (TEM) was used to image control samples on carbon coated copper grids with a Phillips CM200 (FEG) TEM at 200 keV, using the digital micrograph software. EDX spectra were recorded and analyzed using an Oxford Instruments INCA EDX system and Gatan Imaging Filter. Particle density was calculated by counting the number of particles per area for 5 different representative images of each sample, and the quoted error on this is one standard deviation of these data. Grain size was measured using Image J^[2] to record the length and width of ≈400 particles from representative images for each sample. The average diameter for each particle was binned into ≈20 bins, and these data fitted with Gaussian distributions using the Gaussian peak fitting tool in Origin, and the error quoted is the full width half maximum of the fit. The aspect ratio was also binned into ≈20 bins, and fitted with asymmetric distributions using the Asym2sig fitting tool in Origin. The average aspect ratio (error

one standard deviation) was also calculated. In both TEM and SEM images it is only possible to measure two dimensions (i.e. x and y) of the particles. As such, all data presented on grain size and shape excludes information regarding the z dimension.

X-ray Diffraction (XRD): Spectra were recorded using a Bruker-AXS D8 series 2 diffractometer, set to a Bragg Brentano Parafocussing Geometry. X-rays were generated at room temperature using a Cu-K α source at 40 kV. Monochromated X-rays pass through a 2 mm exit slit and an automatic divergence slit of 0.2°. Diffraction intensity was collected at 2θ between 10° and 80° on a Braun position sensitive detector (0.01° and 7.5 seconds per step). These data were processed using AXS Commander and EVA software. These data were smoothed using the Savitzky-Golay signal processing tool in Origin (5 points of window and a polynomial order of 2) to reduce noise generated by the small step size of the diffraction measurements (unsmoothed data shown in **Figure S4** and used to create **Table S1**).

Vibrating Sample Magnetometry (VSM): The biomineralized sample was mounted onto a sample holder and centered to maximize the signal from the magnetic surface to the pick-up coils. Hysteresis loops were measured perpendicular to the surface with an Oxford Instruments Maglab VSM, using an applied field of -10 to 10 kOe at 295 K. It was not possible to measure a signal from a parallel orientated sample as it was not possible to center the sample and take a measurement. The expected saturation magnetization (M_{s_sample}) was calculated as follows:

$$M_{s_sample} = N_{particles} * V_{particle} * A_{sample} * M_{s_CoPt}$$

Where $N_{particles}$ is the number of particles per unit area (**Table 1**), $V_{particles}$ is the volume of a biotemplated CoPt MNP (calculated from the diameter shown in **Table 2**), A_{sample} is the area of the sample (1 cm²) and M_{s_CoPt} is the saturation magnetization of L1₀ cobalt platinum at room temperature (859 emu cm⁻³).^[3]

Magnetic Force Microscopy (MFM): Plots were recorded using magnetized MFM tips (Cr/Co coated MESP, Bruker) on a Multimode Nanoscope III. The topographical height of the surface was recorded in tapping mode at the resonant frequency of the cantilever. This height was then followed

at a lift height above the height of the particles (25-50 nm) to avoid impacts, and thus record magnetic interactions between the particles on the surface and the magnetized tip (see diagram in Figure S9). These MFM data were processed (flattened and scale limits set) using WSxM,^[4] and 3D plots generated in 'R' using the rgl package.

Supporting Figures and Tables

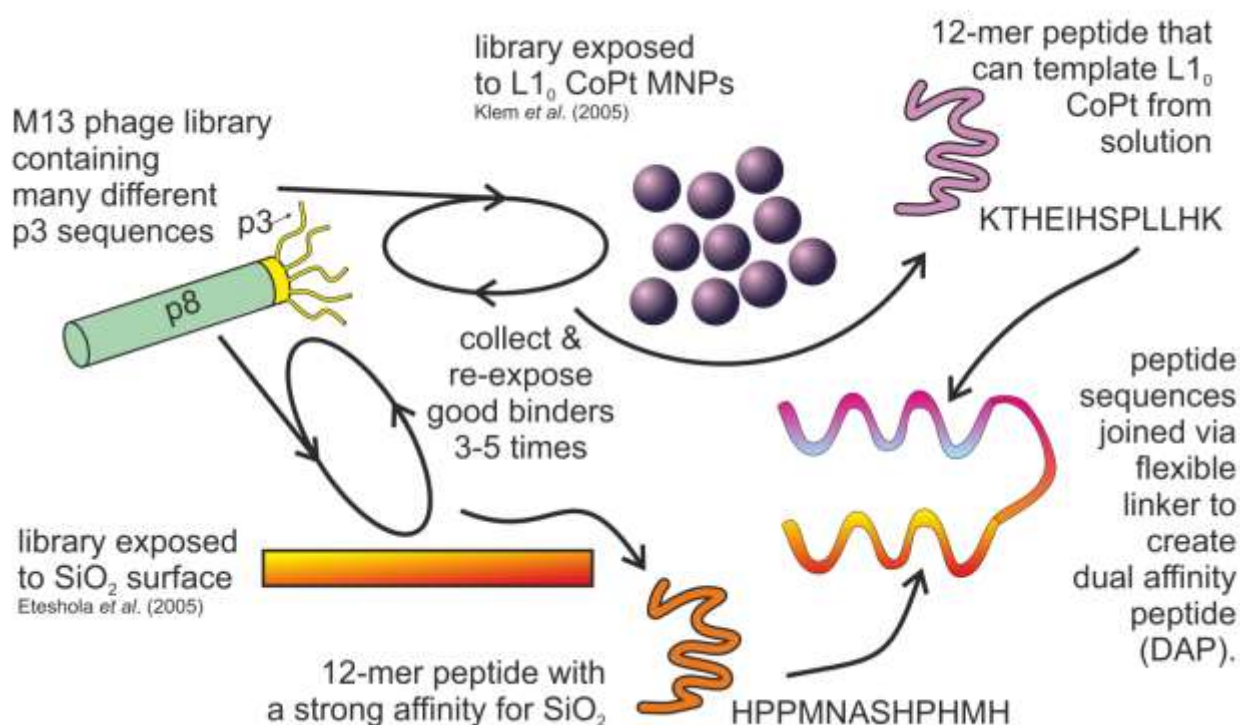


Figure S1. Schematic representation of dual affinity peptide (DAP) design process for the L1₀ CoPt biotemplating dual affinity peptide for use in the biomineralization of magnetic CoPt nanoparticles onto silicon surfaces. Phage display libraries were exposed to two different targets: L1₀ CoPt by Klem *et al.*^[5] and SiO₂ by Eteshola *et al.*^[6] Good binders for the target were collected, amplified and re-exposed to the target for a few rounds. This significantly enriches the library in peptide motifs that have a strong binding affinity for the target. Klem *et al.*^[5] demonstrated that their biopanned peptide (KTHEIHSPLLHK) was able to template cobalt platinum from an aqueous solution. Eteshola *et al.*^[6] demonstrated that their peptide (HPPMNASHPHMH) has a strong binding affinity for thermally grown silicon oxide, cleaned silicon wafer (native oxide) and silica. We joined these two peptides via a flexible linker (GSG) to create a dual affinity peptide (CoPt_DAP, HPPMNASHPHMH-GSG-KTHEIHSPLLHK). The CoPt_DAP is able to bind to the native oxide layer on a cleaned silicon wafer and biotemplate L1₀ CoPt from aqueous solution at room temperature.

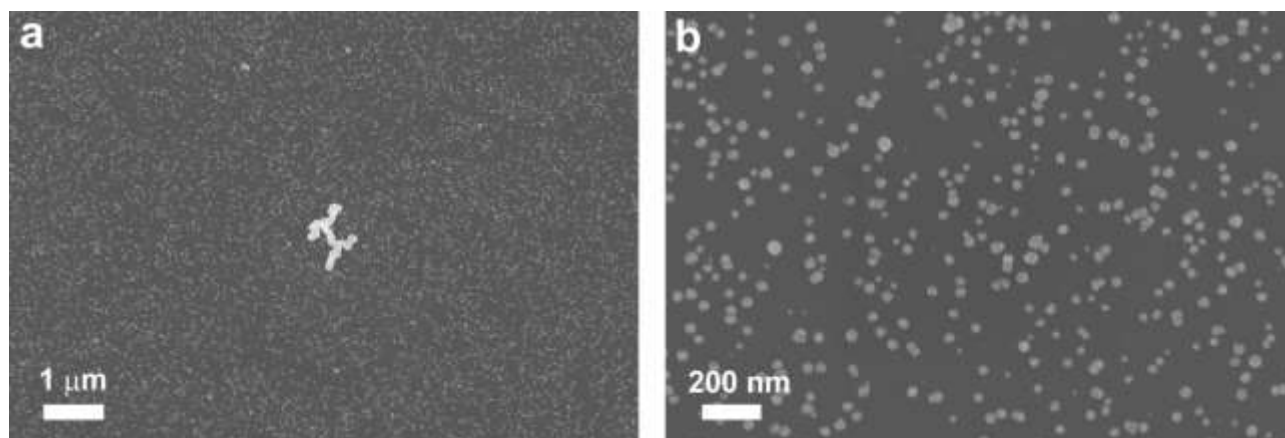


Figure S2. SEM images of samples functionalized with CoPt_DAP from a buffered solution. Clean silicon substrates were immersed in 1 mg mL^{-1} of PBS buffered dual affinity peptide solution, incubated for 1 hour and rinsed with MilliQ water prior to mineralization. a) A representative SEM image of the CoPt_DAP solution incubated sample shows that a sparse distribution of nanoparticles has been biotemplated onto the peptide functionalized surface. b) Close up of the same surface clearly showing how sparsely distributed the particles are. It is likely that the surface is not heavily functionalized with the biotemplating peptide by immersion in a buffered solution, which leads to few particles being biotemplated onto the surface during metallization.

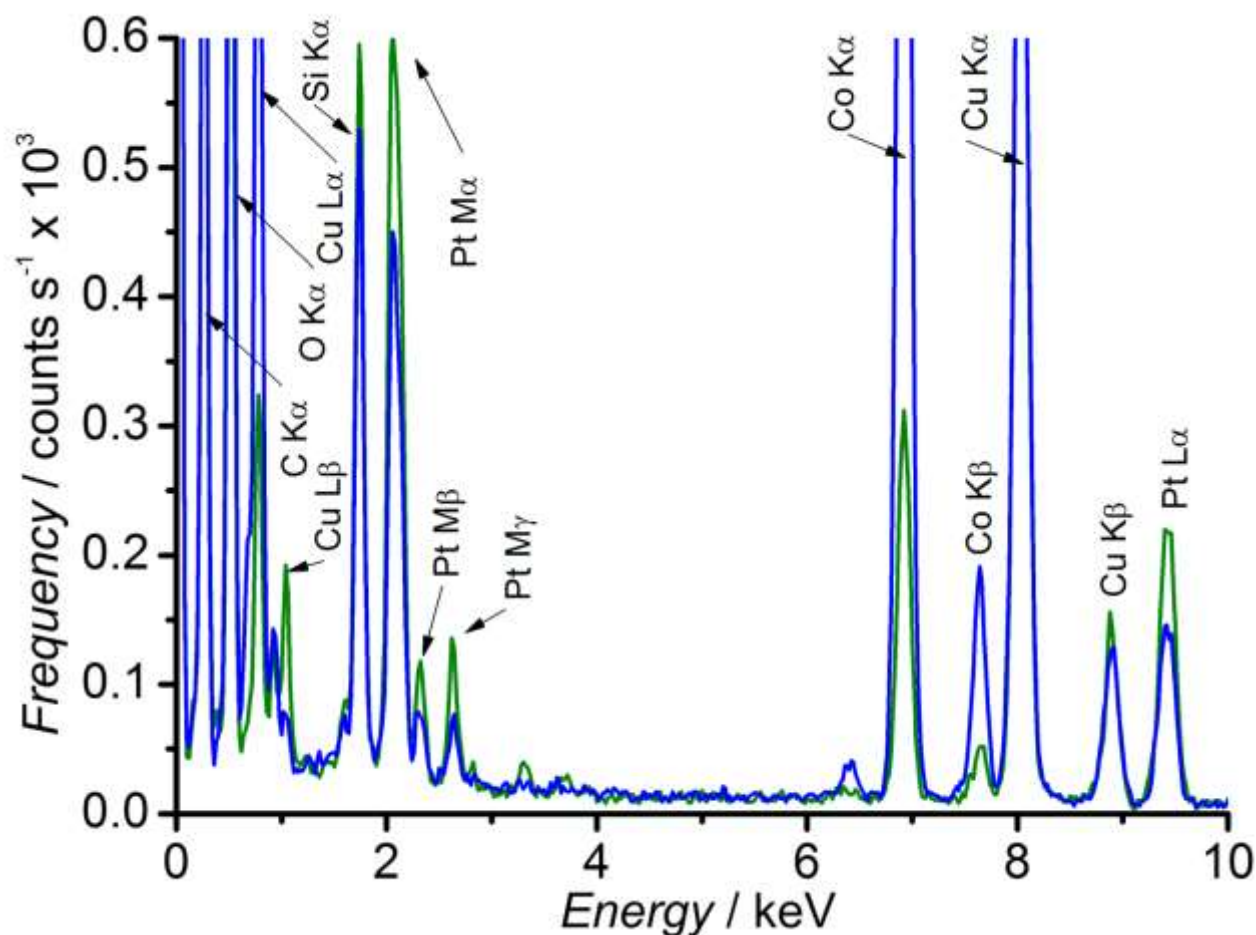


Figure S3. Energy dispersive X-ray (EDX) spectra of bulk templated particle controls from the transmission electron microscope (TEM). Both spectra show peaks from the carbon coated copper grids on which particles are mounted for TEM imaging. Quantification of the Co:Pt atomic ratio in bulk templated particles (**blue**) reflects the stoichiometry of the mineralization solution ($\approx 75:25$). However, the Co:Pt ratio in peptide templated bulk particles (**green**) there is a higher proportion of platinum (46:54), which is very close to the 1:1 ratio required for $L1_0$ CoPt.

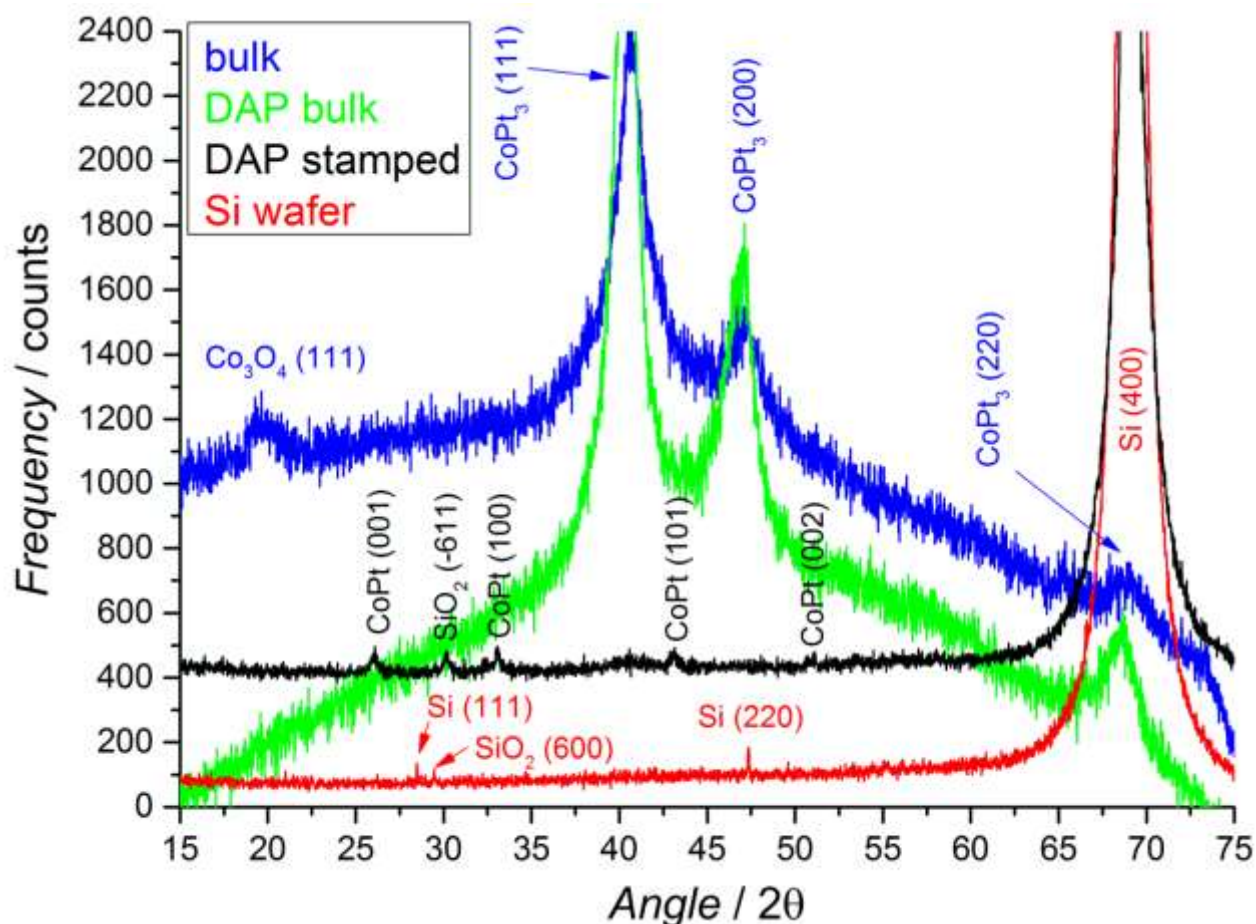


Figure S4. Powder X-ray diffraction (XRD) data for peptide biotemplated CoPt and appropriate controls without smoothing. Bulk precipitated (blue) and bulk peptide biotemplated (green) particles show strong peaks for CoPt_3 , which is not the desired high coercivity L_{10} phase of CoPt. The clean silicon surface (red) shows some oxidation of silicon, most likely from the cleaning process. The surface biotemplated particles (black) show peaks for L_{10} cobalt platinum. Scans are arbitrarily offset on the vertical scale for clarity, details of peak assignments are shown in **Table S1**.

Table S1. Details of peaks measured using XRD. For each sample, the peak position was measured and converted to a d spacing using Braggs Law ($n\lambda = 2d\sin\theta$) where n is 1, λ is the wavelength of the incident X-rays (1.5406 Å), d is the spacing between the planes in Å, and θ is the angle between the incident ray and the scattering planes in radians. Lattice planes are assigned based on comparison of the calculated d spacing from the measured spectra (see Figure 5) to the JCPDS data base, and the nearest match used to assign the material and hkl lattice plane represented by that peak.

sample	2θ [°]	d_{measured} [Å]	$d_{\text{reference}}$ [Å]	compound name	h	k	l	formula	JCPDS No.
bulk	19.40	4.57	4.60	cobalt oxide	1	1	1	Co ₃ O ₄	00-042-1467
	40.87	2.21	2.22	cobalt platinum	1	1	1	CoPt ₃	00-029-0499
	47.05	1.93	1.93	cobalt platinum	2	0	0	CoPt ₃	00-029-0499
	68.83	1.36	1.36	cobalt platinum	2	2	0	CoPt ₃	00-029-0499
DAP bulk	40.41	2.23	2.22	cobalt platinum	1	1	1	CoPt ₃	00-029-0499
	47.05	1.93	1.93	cobalt platinum	2	0	0	CoPt ₃	00-029-0499
	68.60	1.37	1.36	cobalt platinum	2	2	0	CoPt ₃	00-029-0499
DAP 10	25.80	3.45	3.68	cobalt platinum	0	0	1	CoPt	00-029-0498
inks	30.18	2.96	2.97	silicon oxide	-6	1	1	SiO ₂	00-051-1380
surface	33.13	2.70	2.68	cobalt platinum	1	0	0	CoPt	00-029-0498
	40.52	2.22	2.22	cobalt platinum	1	1	1	CoPt ₃	00-029-0499
	43.11	2.10	2.17	cobalt platinum	1	0	1	CoPt	00-029-0498
	51.02	1.79	1.84	cobalt platinum	0	0	2	CoPt	00-029-0498
	69.03	1.36	1.36	silicon	4	0	0	Si	00-027-1402
Si wafer	28.43	3.14	3.14	silicon	1	1	1	Si	00-027-1402
	29.47	3.03	3.04	silicon oxide	6	0	0	SiO ₂	00-051-1380
	47.32	1.92	1.92	silicon	2	2	0	Si	00-027-1402
	69.02	1.36	1.36	silicon	4	0	0	Si	00-027-1402

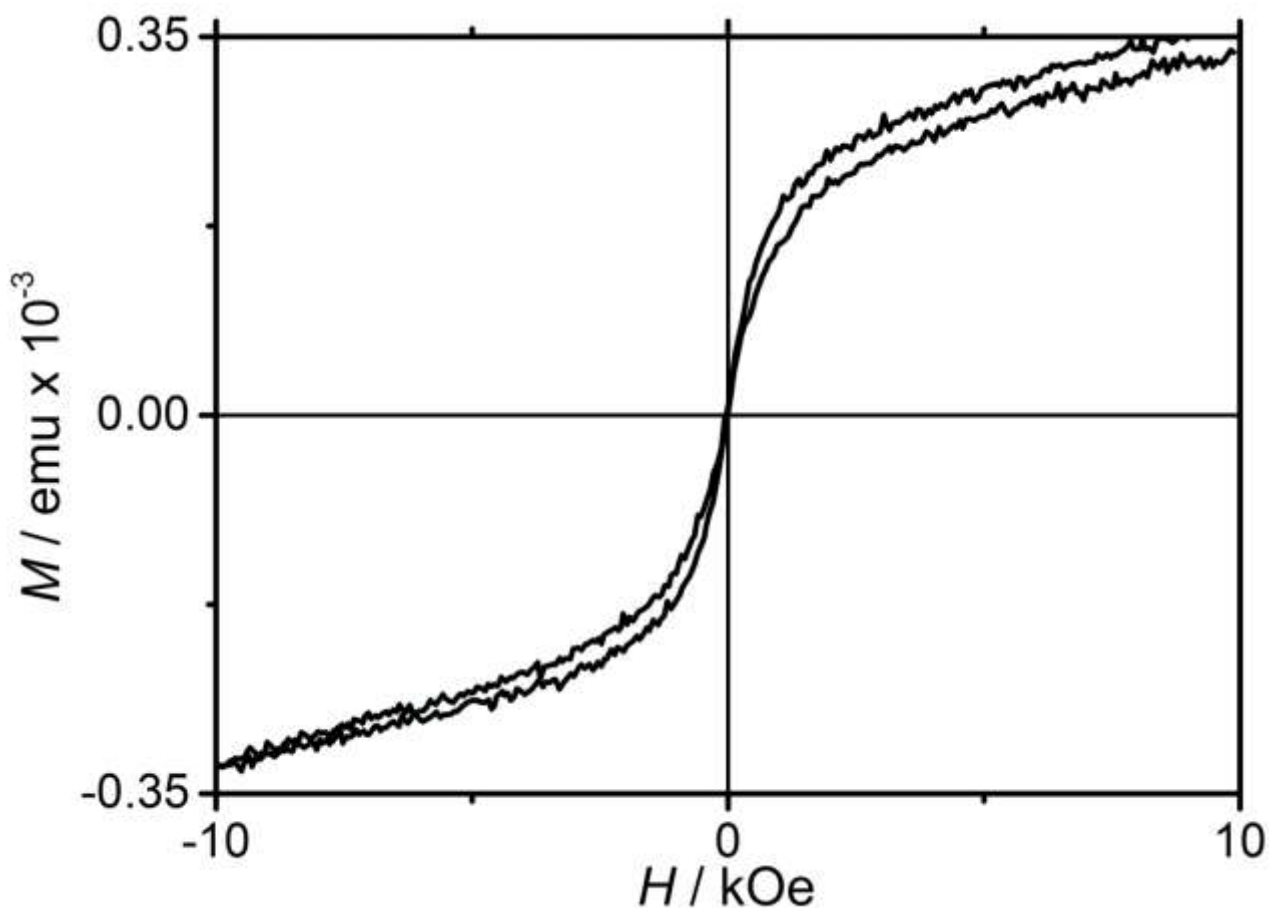


Figure S5. Vibrating sample magnetometry (VSM) was used to record a hysteresis loop for the silicon surface biotemplated CoPt at 295 K perpendicular to the surface. The magnetic signal from the surface is small, but there is a measurable saturation magnetization from the sample ($\approx 3 \times 10^{-4} \text{ emu}$ for a 1 cm^2 sample) that is in the order estimated from the expected volume of material on the surface ($1.6 \times 10^{-4} \pm 0.4 \times 10^{-4} \text{ emu cm}^{-2}$). It was not possible to record any signal parallel to the biotemplated film (see VSM Method in the Supporting Information).

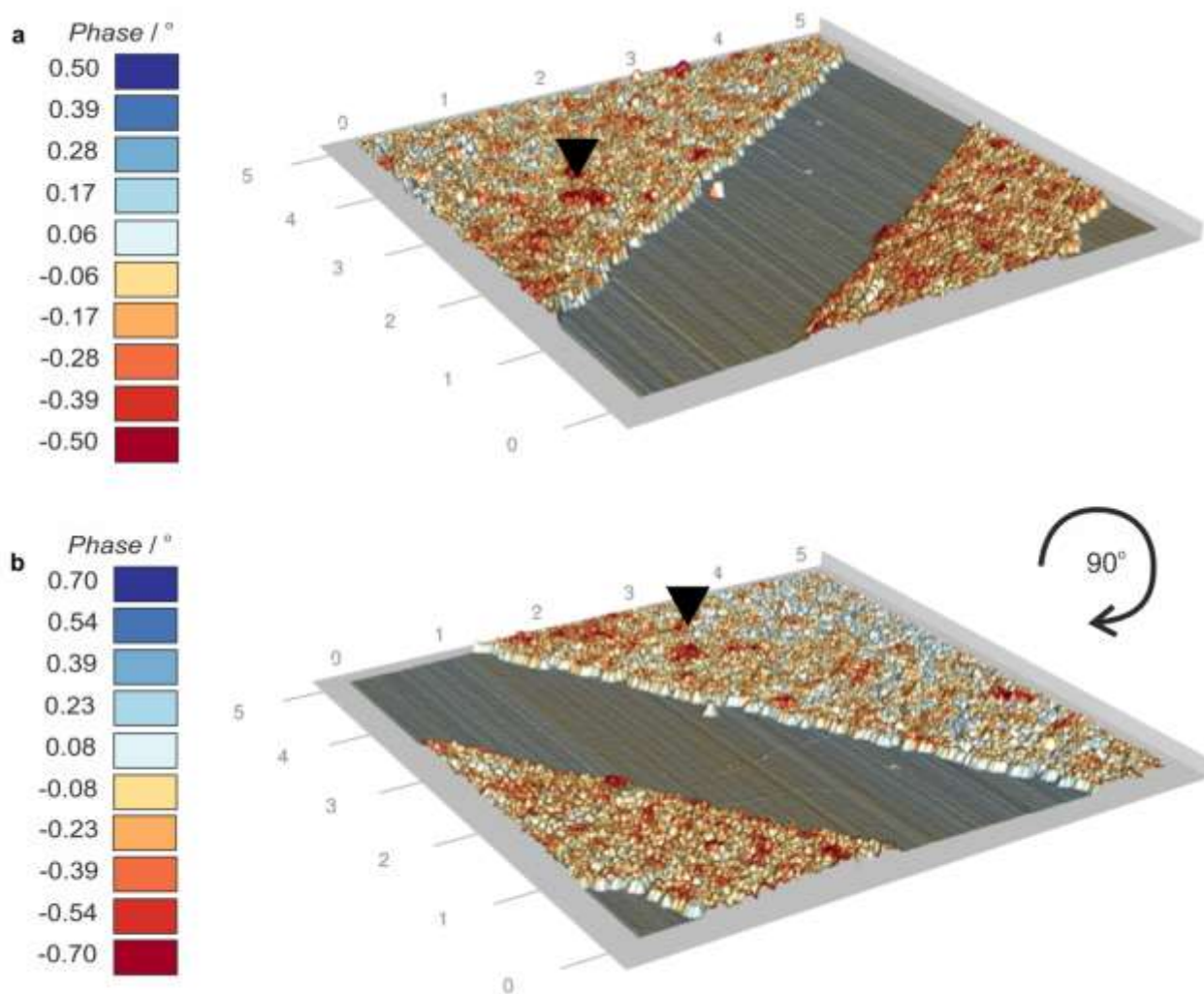


Figure S6. Magnetic force microscopy plots of biotemplated cobalt platinum. Topography recorded in tapping mode (particle height $\approx 25\text{nm}$) and magnetic interactions between the tip and the surface recorded in non-contact mode, at a lift height of 25 nm to avoid tip impacts introducing artefacts (separate scans shown in Figure S8). a) $5\ \mu\text{m}^2$ scan area across abraded section to show silicon surface (center) and magnetic nanoparticles and b) the same area scanned at a 90° angle. Each plot has its own scale for non-contact mode, showing phase shift induced in the resonant peak of the cantilever due to interactions between the magnetized tip and the surface (red is attraction, blue is repulsion). In both plots, multi-particle zones of magnetic attraction and repulsion can be seen, which are independent of topographical height. These position and size of these zones remains stable when the imaging direction is rotated. For example, black triangles highlight the same area of attraction in both plots.

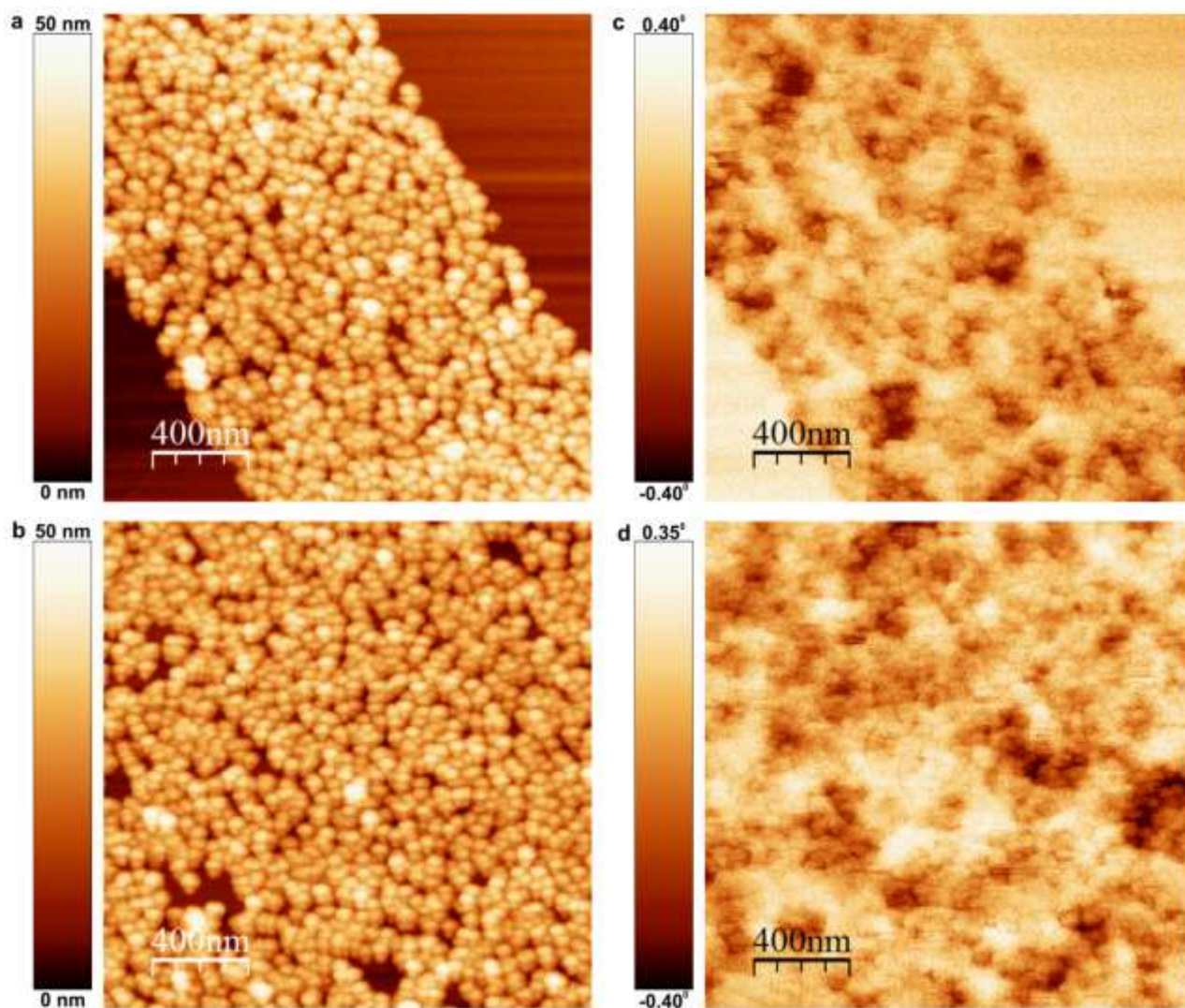


Figure S7. Magnetic force microscopy plots of surface biotemplated cobalt platinum, the same as shown in Figure 6, but topography and phase shift shown separately with individual scale bars. a,b) Topography recorded in tapping mode (particle height ≈ 25 nm) of two different areas and c,d) their respective magnetic plots showing magnetic interactions between the tip and the surface for the same areas. The magnetic interactions are recorded in non-contact mode, at a lift height of 25 nm to avoid tip impacts introducing artefacts. a,c), $2 \mu\text{m}^2$ scan area across abraded section to show silicon surface (edges) and magnetic nanoparticles (center) and b,d) a different area that is not abraded.

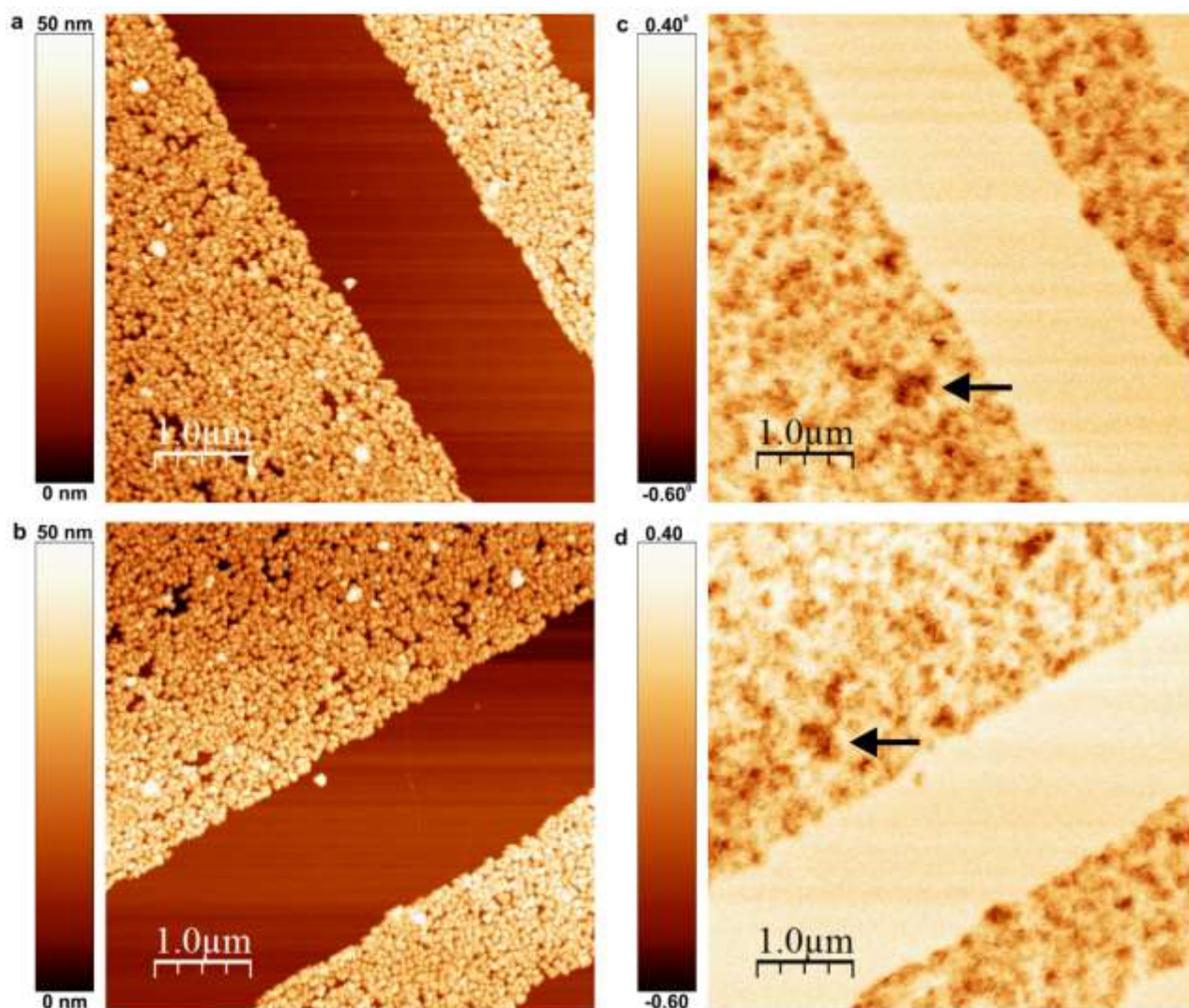


Figure S8. Magnetic force microscopy plots of surface biotemplated cobalt platinum, the same as shown Figure S6, but topography and phase shift shown separately with individual scale bars. a,b) Topography recorded in tapping mode (particle height ≈ 25 nm) and magnetic interactions between the tip and the surface. c,d) Plots recorded in non-contact mode, at a lift height of 25 nm to avoid tip impacts introducing artefacts. a,c) $5 \mu\text{m}^2$ scan area across abraded section to show silicon surface (center) and magnetic nanoparticles (edges), and b,d) the same area scanned at a 90° angle. In both plots, multi-particle zones of magnetic attraction and magnetic repulsion can be seen, which are independent of topographical height. These zones remain stable when the imaging direction is rotated. For example, black arrows highlight the same area of attraction in both plots.

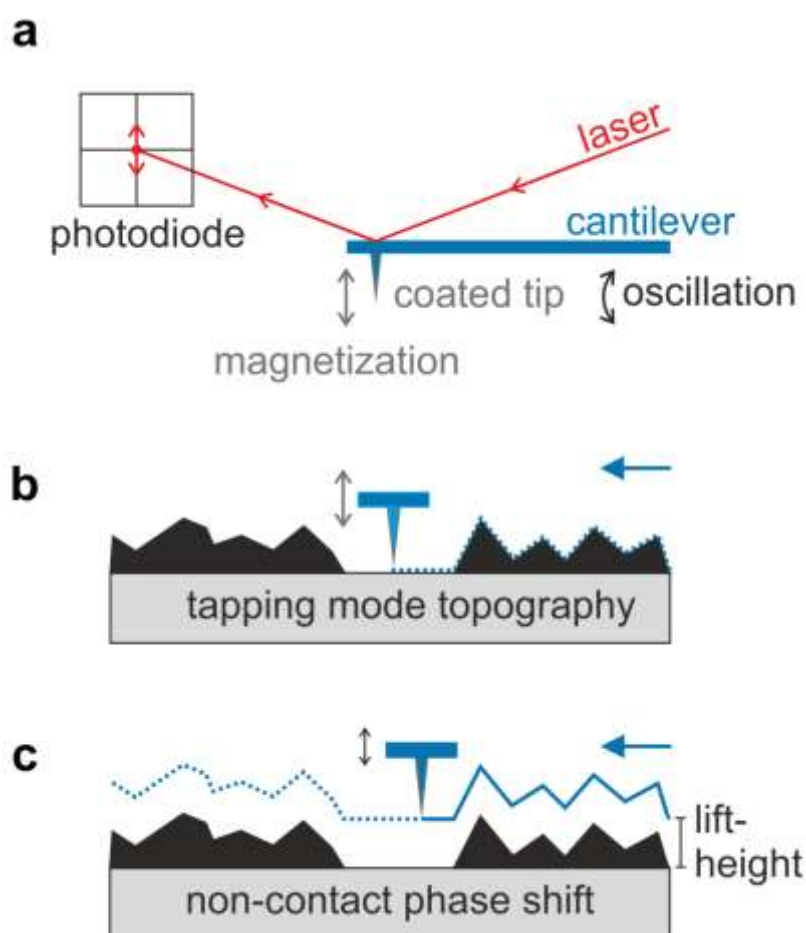


Figure S9. Diagram to show the recording of plots using magnetic force microscopy (MFM). a) A MESP cantilever has a sharp probe (20-30 nm tip diameter) coated in magnetizable Co/Cr. The tip is magnetized perpendicular to the cantilever, and mounted on a piezoelectric head. A laser is reflected off the back of the cantilever and focused onto a photodiode detector. Movement of the tip is detected by the photodiode as the laser point is moved by deflection of the tip. b) The tip is oscillated by the piezo head and tuned to the resonant frequency of the cantilever. This allows the tip to tap across the surface at this resonant frequency, and deflections of the cantilever alter the position of the laser on the photodiode, allowing the recording the topography line-by-line. c) The tip is then lifted to a defined height above the surface, and the topography followed at this fixed distance. Magnetic attraction causes a negative phase shift in the oscillation of the cantilever, and repulsion causes a positive phase shift, thus probing the magnetic interactions between the surface and the tip at a fixed distance.

Supporting Information References

- [1] J. Y. Lim, H. J. Donahue, *Tissue Eng.* **2007**, *13*, 1879.
- [2] M. D. Abramoff, P. J. Magalhaes, S. J. Ram, *Biophotonics Int.* **2004**, *11*, 36.
- [3] M. Yu, H. Ohguchi, A. Zambano, I. Takeuchi, J. P. Liu, D. Josell, L. A. Bendersky, *Mat. Sci. Eng. B* **2007**, *142*, 139.
- [4] I. Horcas, R. Fernandez, J. M. Gomez-Rodriguez, J. Colchero, J. Gomez-Herrero, A. M. Baro, *Rev. Sci. Instrum.* **2007**, *78*, 013705.
- [5] M. T. Klem, D. Willits, D. J. Solis, A. M. Belcher, M. Young, T. Douglas, *Adv. Funct. Mater.* **2005**, *15*, 1489.
- [6] E. Eteshola, L. J. Brillson, S. C. Lee, *Biomol. Eng.* **2005**, *22*, 201.